European Geothermal Congress 2013
Pisa, Italy, 3-7 June 2013

A novel multi-tube heat exchanger applicable for a geothermal power plant

J.C.Hsieh[1], T.R. Guo[1], Y.R. Lee[1], L.W. Liu[1]

P.Y.Cheng[2], C.C.Wang[2]

[1] Green Energy and Environment Research Laboratories, Industrial Technology Research Institute

[2] Department of Mechanical Engineering, National Chiao Tung University, [2]EE513, 1001 University Road, Hsinchu, Taiwan 300

[2]002-886-3-5131479, [2]pao70133@yahoo.com.tw

Keywords: Downhole heat exchanger, Geothermal, Organic Rankine Cycle, Shell and Tube heat exchanger

ABSTRACT

. In this study, the present authors had proposed a novel multi-tube heat exchanger (NMTHE) to retrieve geothermal energy as the heat source for ORC. The NMTHE was designed to be placed in the well and it features the shell and tube heat exchanger configuration. The tube-side fluid flow has been divided into 40 small tubes (small tubes with outer diameter 12.7 mm and inner diameter 10.7 mm). The 40 small tubes are designed at manifold to improve flow uniformity in the well. The NMTHE was designed subject to natural convection in the shell-side and forced convection on the tube-side. The total manifold length of the heat exchanger is 11 meters and the effective heat exchange area is 17.22 m².The inlet temperature of the heat exchanger tube-side is 100.4 °C, the outlet temperature is 130 °C, flow rate is 10 tons/hr and the estimated heat capacity is 250 kW, which is used as the heat input into the ORC system to generate electricity. Through this design, we can improve the effective heat capacity within limited space in the well.

The preliminary experiment showed that by increasing the flow rate of pure water to 13 ton/hr, the heat transfer rate would be as large as 700 kW. The inlet and the outlet temperature of the heat exchanger shell-side is around 80~85 °C and 120~130 °C, respectively. Test results also shows that the shell-side heat transfer coefficient peaks at 1600 W/m^2 K when the inlet pressure is 1.5bar at the flow rate 7.4 CMH and is decreased to 800 W/m^{2}K 2.57bar at 6.6 CMH. It is noted that the pressure of the hot water from the geothermal well affects the heat transfer coefficient due to the effects of vapour quality and dissolved carbon dioxide. Moreover, heat transfer coefficient is increased with the high flow rate for geothermal water. The novel

multi-tube heat exchanger associated with an ORC system has been successfully operated with a maximum capacity of 60 kWh.

NOMENCLATURE

NMTHE	novel multi-tube heat exchanger	ρ	density
ORC	Organic Rankine Cycle	V	characteristic velocity
Q	heat exchange rate	D	characteristic length
U	overall heat transfer coefficient	μ	fluid viscosity
A	effective heat transfer area	g	gravity
LMTD	logarithm mean temperature difference	β	expansion coefficient
h_i	tube-side heat convection coefficient	C_p	specific heat
A_i	tube-side effective heat exchange area	CMH	cubic meters per hour
h_o	shell-side heat convection coefficient	E_g	power generation
A_o	shell-side effective heat exchange area	T_1	temperature difference of the shell-side
R_w	heat exchanger wall resistance	T_2	temperature difference of the tube-side
Qt	heat extraction	**SUBSCRUPT**	
Nu	Nusselt number	i	tube-side
Pr	Prandtl number	o	shell-side
Re	Reynolds number	w	heat exchanger wall
Ra	Rayleigh number	f	working fluid
f	friction factor	s	surface
d	diameter	∞	environment
k	heat conduction coefficient	D	under characteristic length

1. INTRODUCTION

Clean energy has enjoyed its popularity for the past few decades. It is not only eco-friendly but can also be perpetually operated. Geothermal energy is one of the typical kinds of clean energy. In normal operation, it extract heat out of the well via certain heat exchangers in the form such as single U-pipe, double U-pipe, simple co-axial, and complex coaxial (1). There had been appreciable studies concerning the performance of the ground heat exchangers, including numerical analysis (2-3), experimental verification (4-5), field testing (6-7) and thermal response (8-11).

In this study, a novel multi-tube heat exchanger is proposed and integrated with the geothermal power plant. The working fluid in the tube-side of the heat exchanger is pure water, where in the shell-side the working fluid is geothermal hot water. The geothermal heat exchanger is used to extract heat from the well and is then integrated as the heat source into an organic power cycle to generate electricity. The working fluid for the organic Rankine cycle is pentafluoropropane, also known as R-245fa. The heat extraction, power generation and ORC efficiency will be examined in this study.

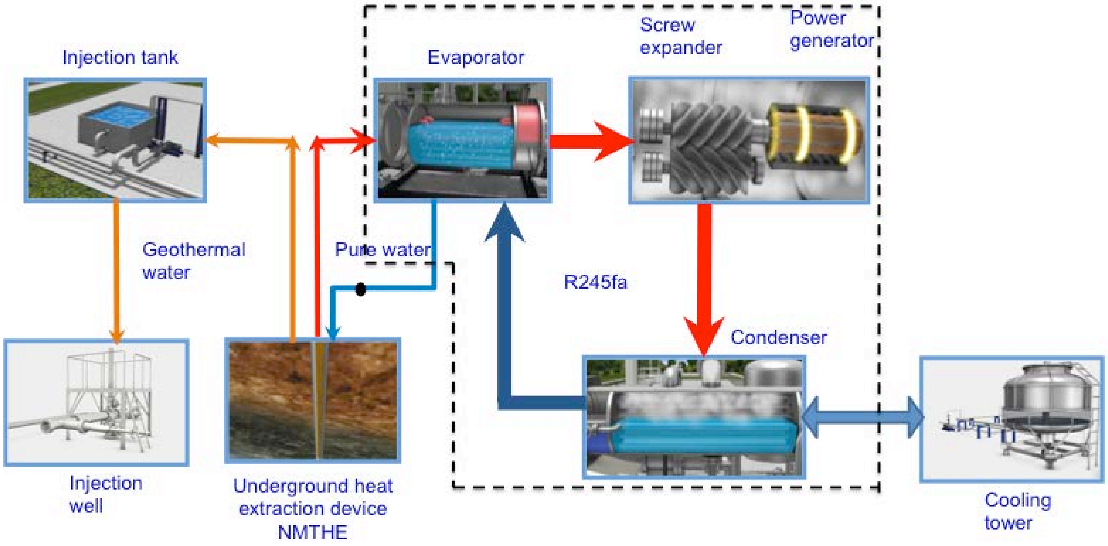

Figure 1: Schematic figure of the heat exchanger system and the ORC system

2. EXPERIMENT

In Taiwan, there are abundant resources of geothermal energy in I'Lan, where geothermal energy is utilized to generate electricity along with the Organic Rankine Cycle (ORC). The system is capable of delivering an electric power of 60 kWh. The prototype of the NMTHE design is improved.

To avoid the influence of water quality, a two-stage heating system is designed in the geothermal heat exchanger system as shown in Fig. 1. It contains a geothermal loop and an ORC loop. In the geothermal system, the production well erupts geothermal water which exchange heat in the NMTHE with the pure water in the ORC system. The high temperature pure water then enters into the evaporator of the ORC system to heat R-245fa, and then flows back to NMTHE to complete a full cycle.

In the ORC system, refrigerant is evaporated and flows into the screw expander to deliver work output, the refrigerant then condenses by the water where it was further cooled by an additional cooling tower. In order to evaporate the refrigerant, the pure water that is utilized for heating is designed to have an inlet temperature above 120 °C with a flow rate of 13 tons per hour. In this experiment, four different cases have been tested.

The main purpose of this experiment is to exchange heat from underground in order to facilitate the ORC system. There are three types of conventional borehole heat exchangers, which are the U-pipe heat exchanger, spiral (helical) heat exchanger and the multi-tubes (shell and tube like) heat exchanger, respectively. Normally the shell and tube heat exchangers have a larger heat exchange rate, but the shape of the heat exchanger sometimes may incur some flow mal-distribution, and this mal-distribution can be appreciably reduced through the exploitation of small tubes as proposed in this study. Some further details describing the on-site test facility are giving in the following.

2.1 Geothermal well

The heat exchanger is designed to extract heat of 250 kW from a 200-meter underground. Prior to the experiment, the geological measurement of the temperature variation of the geothermal water is conducted as shown in Fig. 2. It appears that at 200-meter underground the temperature is around 135~140 °C. The geothermal water contains saturated water and steam, also some carbon dioxide with concentration around 2~4%. Originally the heat exchanger was designed to operate underground, but in actual operation, it is used at the surface level to make use the erupted geothermal water.

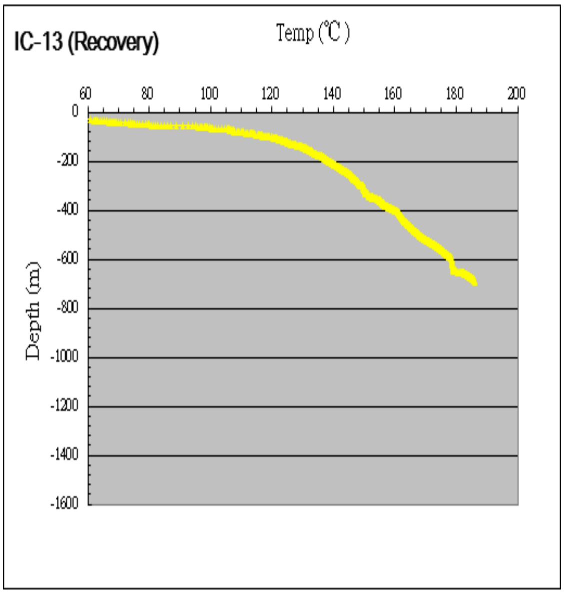

Figure 2: Temperature distribution in I'Lan.

2.2 Multi-tube heat exchanger (NMTHE) design

The heat exchanger is comprised a counter flow arrangement due. The required tube-side water temperature inlet and outlet is 100.4 °C and 130 °C, respectively. Details of the heat exchanger design is given as follows based on Wang (12), hence the dimensions for the heat exchanger can be determined.

$$\mathrm{LMTD} = \frac{\Delta T_1 - \Delta T_2}{\ln(\frac{\Delta T_1}{\Delta T_2})} \quad [1]]$$

$$\mathrm{Q} = \mathrm{UA} * \mathrm{LMTD} \quad [2]$$

According to Eqs. [1] and [2] , the overall conductance UA can be obtained, and the reciprocal of UA represents the overall thermal resistance which is consisted of separate resistances in tube-side, wall, and shell-side, respectively:

$$\frac{1}{\mathrm{UA}} = \frac{1}{\mathrm{h_i A_i}} + \mathrm{R_w} + \frac{1}{\mathrm{h_o A_o}} \quad [3]$$

The tube-side resistance can be easily obtained from the well know Gnielinski correlation (13):

$$\mathrm{Nu} = \frac{\mathrm{h_i d_i}}{\mathrm{k_f}} = \frac{(f/2)*(\mathrm{Re}-1000)*\mathrm{Pr}}{1.07+12.7*\sqrt{f/2}*(\mathrm{Pr}^{2/3}-1)} \quad [4]$$

$$\mathrm{f} = (1.58 \ln \mathrm{Re} - 3.28)^{-2} \quad [5]$$

$$\mathrm{Re} = \frac{\rho * V * D}{\mu} \quad [6]$$

And the shell-side heat transfer is regarded natural convection and can be calculated from the Churchill correlation:

$$\mathrm{Ra} = \frac{g\beta(T_s - T_\infty)D^3}{\left(\frac{\mu}{\rho}\right) * \left(\frac{k}{\rho C_p}\right)} \quad [7]$$

$$\mathrm{Nu} = \frac{h_0 d_o}{k_f} = \left(0.6 + \frac{0.387 * \mathrm{Ra_D}^{1/6}}{\left[1 + \left(\frac{0.559}{\mathrm{Pr}}\right)^{9/16}\right]^{8/27}}\right)^2 \quad [8]$$

A preliminary calculation using the aforementioned correlation at the designed condition, the heat transfer coefficient of both tube-side and shell-side is 6093 (W/m^2 K) and 1162 (W/m^2 K), respectively. It is obvious that the dominant resistance is mainly on the shell-side of the heat exchanger On the other hand, the required heat transfer area subject to heat transfer duty is 18.6 m^2.

The foregoing calculation implicates that the dominant resistance is on the shell-side, and it is imperative to reduce the shell-side resistance accordingly. As a consequence, the present study propose a multi-tube design to introduce turbulence at the shell-side. Through the utilization of smaller tubes, both heat transfer and pressure drop can be improved simultaneously. Therefore the final design employs a multi-tube shaped heat exchanger, utilizing small pipes having an internal diameter of 10.7 mm and a 12.7 mm outer diameter. The NMTHE is built up with 40 small pipes and 1 larger pipe with a diameter of 40 mm as shown in Fig. 3, the total length of the heat exchanger is 11 meters, and has an effective heat transfer area of 17.22 m^2. The tube material is cooper and a baffle, as shown in Fig. 4, is used to stably support the small pipes. After the NMTHE is built, sensors are installed and the whole device is placed in a larger duct.

Figure 3: NMTHE

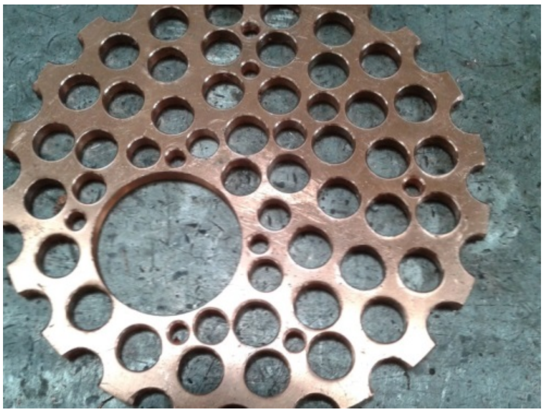

Figure 4: Baffle

2.3 Four cases of experiment

In the experiment, four sets of data have been tested, each with distinct inlet pressure and geothermal water flow rate, shown in Table 1. In each experiment, heat extraction from the NMTHE and power generation from the ORC system is reported. Note that the inlet pressure is actually fluctuating during operation.

Table 1: The four operation conditions of the NMTHE

NMTHE shell-side (geothermal water) Basic operation condition				
	Case1	Case2	Case3	Case4
Inlet pressure (bar)	1.5	3.15	2.57	2.4
flow rate (CMH)	7.4	8.64	6.6	8.64

3. RESULTS AND DISCUSSION

Figures 6-13 shows the heat extraction and power generation and the associated ORC efficiency vs. running time for all four cases. Heat extraction from the geothermal energy is indicated in red and the unit is in kiloWatts (kW). The power generation by the ORC system is indicated in blue and the unit is also in kiloWatts (kW). The second figure in each case is the ORC efficiency, which is defined as

$$\text{ORC efficiency} = \frac{E_g}{Q_t} \qquad [10]$$

As shown in the figures for the first three cases, it is shown that the ORC efficiency is increased with the elapsed of time, while in the fourth case the ORC efficiency, heat extraction and power generation is slightly decreased. In terms of average overall ORC efficiency, it appears that case 2 shows the highest ORC efficiency around 8.6% whereas case 1 shows the lowest efficiency around 8.1%. Basically, the difference is associated with the heat transfer characteristics of the shell-side of the proposed heat exchanger. As tabulated in Table 1, the inlet pressure for case 2 is about 3.15 bar while it is 1.5 bar in case 1, suggesting appreciably difference in the inlet pressure entering the shell-side of the heat exchanger. As mentioned in the experimental section, there is a considerable amount of CO_2 in the shell-side fluid (~4%). As a consequence, higher pressure will renders the CO_2 into a smaller gas bubble which may entrain along the shell-side and cause better mixing and turbulence resulting in a better heat transfer performance and a higher overall ORC efficiency.

3.1 CASE 1

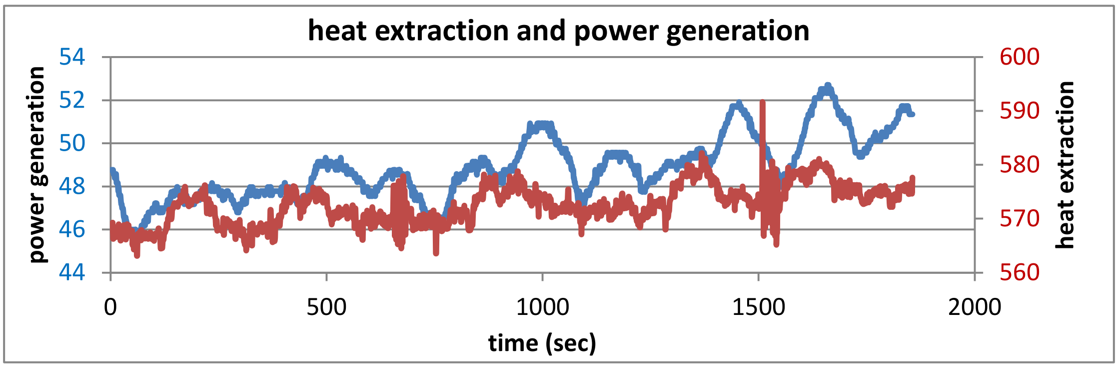

Figure 6: Heat extraction and power generation for case 1.

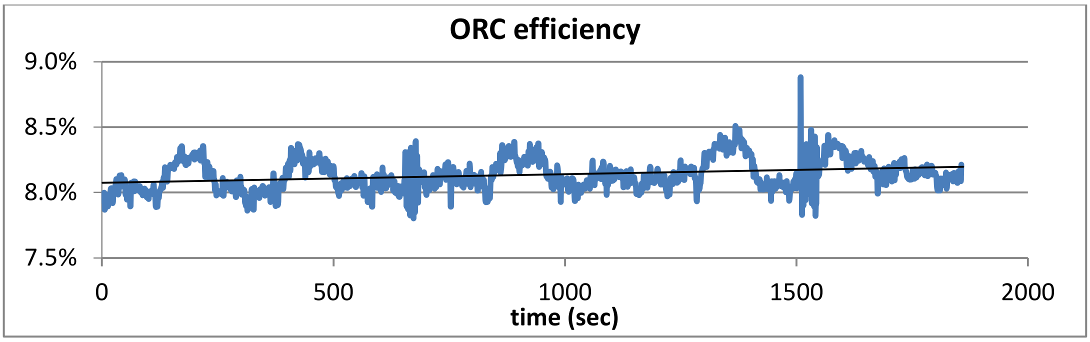

Figure 7: ORC efficiency for case 1.

3.2 CASE 2

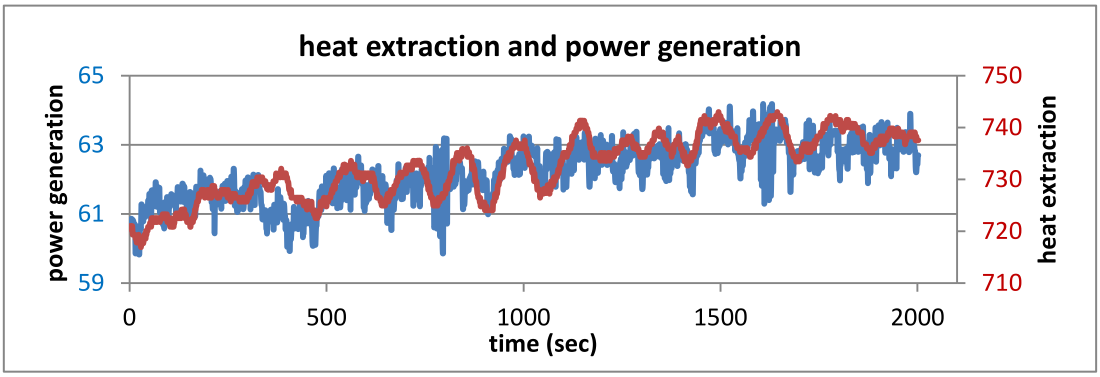

Figure 8: Heat extraction and power generation for case 2.

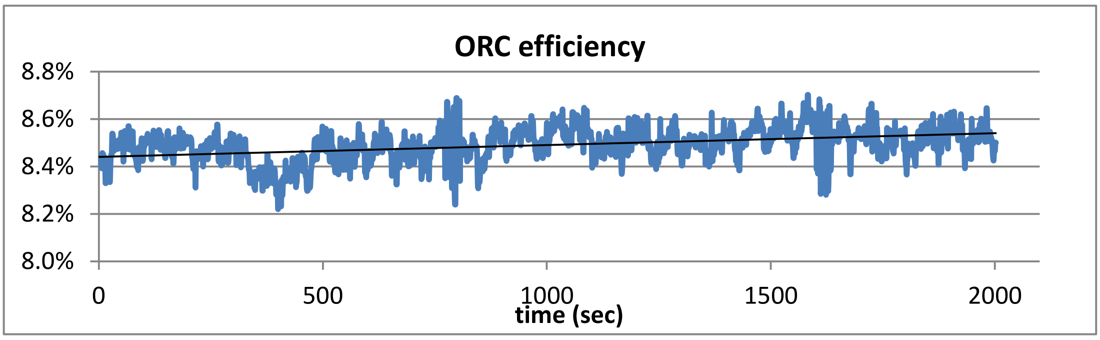

Figure 9: ORC efficiency for case 2.

3.3 CASE 3

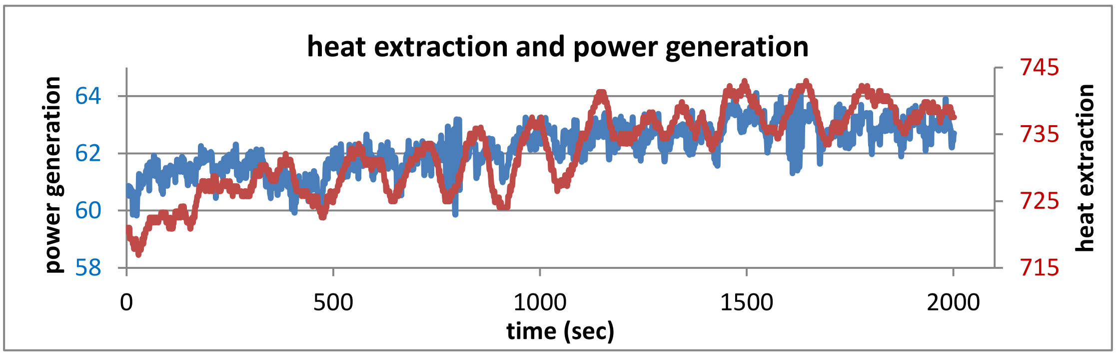

Figure 10: Heat extraction and power generation for case 3.

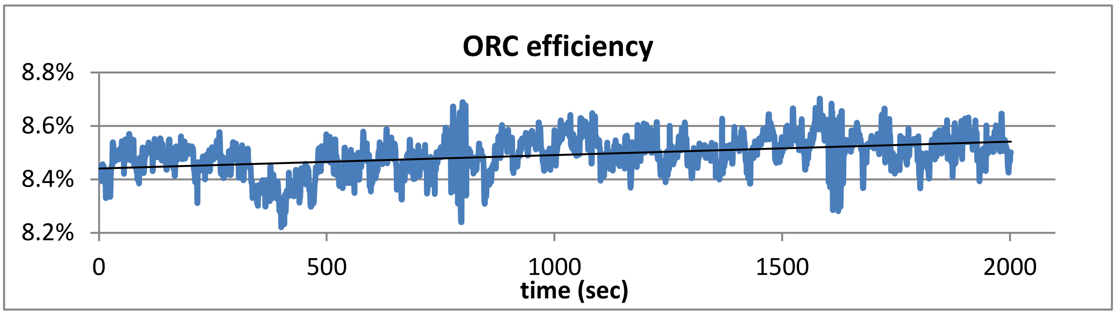

Figure 11: ORC efficiency for case 3.

3.4 CASE 4

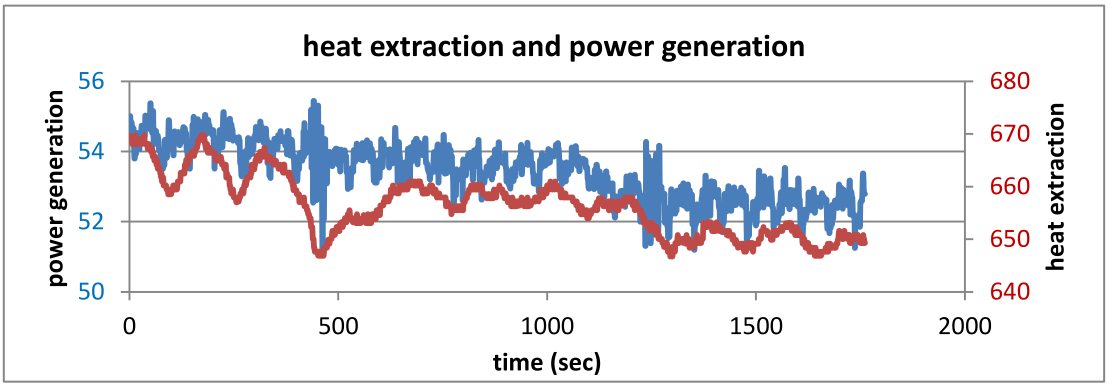

Figure 12: Heat extraction and power generation for case 4.

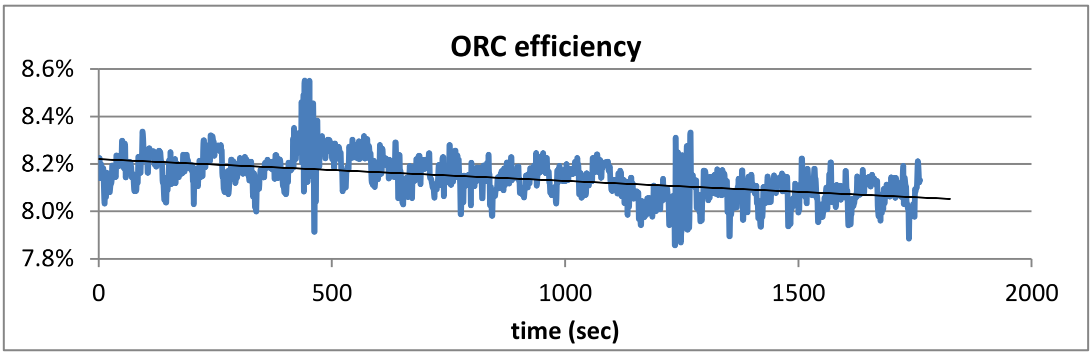

Figure 13: ORC efficiency for case 4.

Normally the efficiency of a Rankine Cycle is related to some important operation parameters. Firstly, lowering the outlet pressure of the turbine, which results in gross net output work. Eventually it leads to an increase of efficiency. Secondly, lowering the outlet temperature of the condenser. The principle is the same as that of lowering the outlet pressure of the turbine: increasing the net output work, in spite of the heat input also increases, the efficiency is still increased. Thirdly, raising the pressure of the evaporator may also increase the overall efficiency. By increasing the pressure inside the evaporator, the heat efficiency is slightly enhanced, accompanying with a slight increase in the outlet pressure of the evaporator.

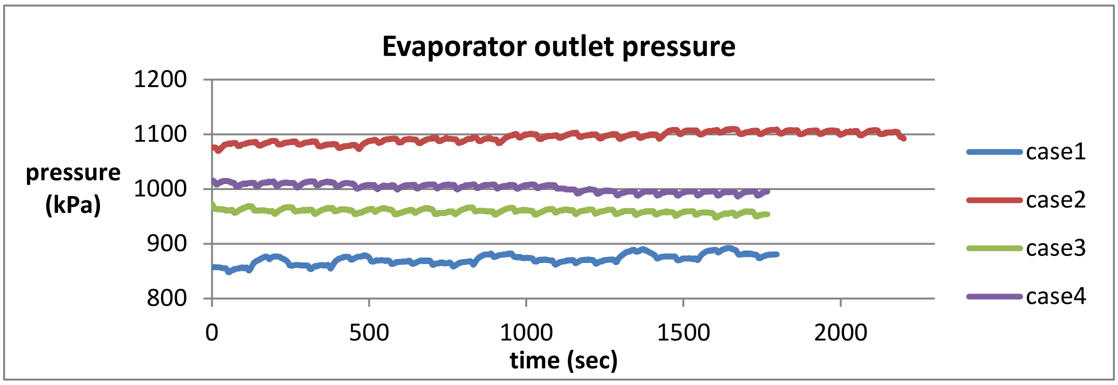

Figure 14: The outlet pressure of the evaporator.

As can be seen in Fig 14, the outlet pressure of the evaporator from case 1 to case 4 shows a slight increase, whereas the outlet pressure decreases in case 4. In this regard, one can see a slight decrease in overall efficiency for the first three cases while a slight increase in efficiency for case 4 is encountered. On the other hand, as depicted in Fig 15., the first three reveals a noticeable increase in the temperature of the evaporator outlet, whereas in case 4 there is no distinct increase in temperature. In summation of the aforesaid reasoning, the ORC efficiency for case 4 shows slight decline.

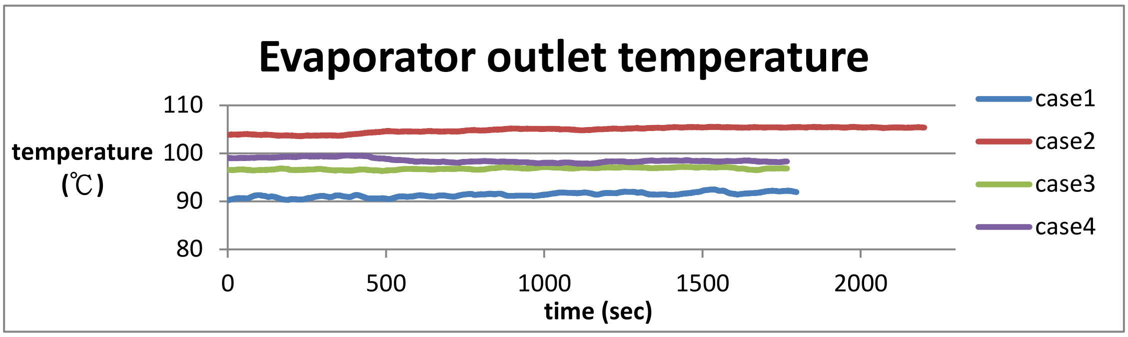

Figure 15: The outlet temperature of the evaporator

4. CONCLUSION

In this study, the performance of a novel multi-tube heat exchanger (NMTHE) incorporated with the ORC system. The heat exchanger characterized small diameter tubes to provide better flow mixing. A total of four cases with varying inlet pressure were reported. Based on the results, the following conclusions can be obtained:

(1) By the eruption of geothermal water, the NMTHE is capable of delivering more than 700 kW of the thermal energy to the ORC system, with the efficiency being around 8~8.6%.

(2) Test results indicated that higher inlet pressure of the NMTHE may give rise to larger system efficiency. This is associated with the higher inlet pressure which leads to a better mixing of the shell-side flow.

(3) A lower condensing temperature and a higher evaporation temperature result in higher system efficiency. It is also found that the system parameters, especially the

evaporation temperature is strongly related to the performance of NMTHE.

REFERENCES

1. G. Florides and S. Kalogirou.: Ground heat exchangers—A review of systems, models and applications, *Renewable Energy*, 32, Cyprus, (2007), 2461–2478.
2. R. Al-Khoury., T. K¨olbel., R. Schramedei.: Efficient numerical modeling of borehole heat exchangers, *Computers & Geosciences*, 36, Germany, (2010), 1301-1315
3. Y. Nam., R. Ooka. S. Hwang.: Development of a numerical model to predict heat exchange rates for a ground-source heat pump system, *Energy and Buildings*, 40, Japan, (2008), 2133-2140
4. A. Pertzborn., S. Hackel., G. Nellis., S. Klein.: Experimental validation of a ground heat exchangers model in a hybrid ground source heat pump, *HVAC&R Research*, 17(6), United States, (2011), 1101-1114
5. K. Lim., S. Lee., C. Lee.: An experimental study on the thermal performance of ground heat exchanger, *Experimental Thermal and Fluid Science*, 31, Korea, (2007), 985-990
6. S. Lazzari., A. Priarone., E. Zanchini.: Long-term performance of BHE (borehole heat exchanger) fields with negligible groundwater movement, *Energy*, 35, Italy, (2010), 4966-4974
7. D. Pahud., B. Matthey.: Comparison of the thermal performance of double U-pipe borehole heat exchangers measured in situ, *Energy and Buildings*, 33, Switzerland, (2001), 503-507
8. A. –M. Gustafsson., L. Westerlund.: Multi-injection rate thermal response test in groundwater filled borehole heat exchanger, *Renewable Energy*, 35, Sweden, (2010), 1061-1070
9. J. Acuña., P. Mogensen., B. Palm.: Distributed thermal response tests on a multi-pipe coaxial borehole heat exchanger, *HVAC&R Research*, 17(6), Sweden, (2011), 1012-1029
10. C. Lee., M. Park., T. B. Nguyen., B. Sohn., J. M.Choi., H. Choi.: Performance evaluation of closed-loop vertical ground heat exchangers by conducting in-situ thermal response tests, *Renewable Energy*, 42, South Korea, (2012), 77-83
11. R. A. Beier., M. D. Smith., J. D. Spitler., Reference data sets for vertical borehole ground heat exchanger models and thermal response test analysis, *Geothermics*, 40, United States, (2011), 79-85
12. C. C. Wang: Heat Transfer Design, *Wunan*, Taipei, (2007).
13. Gnielinski, V., 1976, "New Equation for Heat and Mass Transfer in Turbulent Pipe and Channel Flow," Int. Chem. Eng., Vol. 16, pp. 359-368.

Acknowledgements

The authors are grateful for the supports provided by Bureau of Energy, Ministry of Economic Affairs and Green Energy and Environment Research Laboratories, Industrial Technology Research Institute for National Chiao Tung University.